Sequential firing codes for time in rodent medial prefrontal cortex

Zoran Tiganj

Department of Psychological and Brain Sciences, Center for Memory and Brain, Boston University, USA

Jieun Kim, Min Whan Jung

Center for Synaptic Brain Dysfunctions, Institute for Basic Science and Department of Biological Sciences, Korea Advanced Institute of Science and Technology, Daejeon, Korea

Marc W. Howard

Department of Psychological and Brain Sciences, Center for Memory and Brain, Boston University, USA

Abstract

A subset of hippocampal neurons, known as "time cells" fire sequentially for circumscribed periods of time within a delay interval. We investigated whether medial prefrontal cortex (mPFC) also contains time cells and whether their qualitative properties differ from those in the hippocampus and striatum. We studied the firing correlates of neurons in the rodent mPFC during a temporal discrimination task. On each trial, the animals waited for a few seconds in the stem of a T-maze. A subpopulation of units fired in a sequence consistently across trials for a circumscribed period during the delay interval. These sequentially activated time cells showed temporal accuracy that decreased as time passed as measured by both the width of their firing fields as well as the number of cells that fired at a particular part of the interval. The firing dynamics of the time cells was significantly better explained with the elapse of time than with the animals' position and velocity. The findings observed here in the mPFC are consistent with those previously reported in the hippocampus and striatum suggesting that the sequentially activated time cells are not specific to these areas, but are part of a common representational motif across regions.

Introduction

A variety of brain regions have been implicated in interval timing over the scale of seconds to minutes, including the striatum (see Buhusi & Meck, 2005, for a review) and medial prefrontal cortex (mPFC) (Mangels, Ivry, & Shimizu, 1998; Onoe et al., 2001; Kim, Jung, Byun, Jo, & Jung, 2009). For instance, Kim, Ghim, Lee, and Jung (2013) recently showed that the ensemble state in the medial prefrontal cortex (mPFC) changed gradually

during the delay period of a temporal discrimination task. Critically, Kim et al., 2013 found that the discriminability of the time during the delay that could be computed from the ensemble similarity decreased with time elapsed. Decreasing accuracy with elapsing time is a hallmark of behavioral measures of memory and timing in both human and non-human animals (Lewis & Miall, 2009; Lejeune & Wearden, 2006; Wearden & Lejeune, 2008).

There are many potential mechanisms that could cause a change in accuracy at the ensemble level as time elapses. For instance, a population of neurons whose firing rate changes monotonically as a function of the logarithm of the time during the delay would have this property; Kim et al., 2013 reported a population of units exhibiting this pattern of results. However, there are other alternatives as well. For instance, several labs have reported "time cells" in the hippocampus that fire during circumscribed parts of a delay period (Pastalkova, Itskov, Amarasingham, & Buzsaki, 2008; Gill, Mizumori, & Smith, 2011; Kraus, Robinson, White, Eichenbaum, & Hasselmo, 2013; MacDonald, Lepage, Eden, & Eichenbaum, 2011; Salz et al., 2016). Also, time cells were reported in the striatum (Mello, Soares, & Paton, 2015; Adler et al., 2012). Different time cells fire at different times during the interval, enabling a population of time cells to generate a signal that could be used in interval timing. The width of time cells' firing fields increases with their time of peak firing (Howard et al., 2014; Kraus et al., 2013; Mello et al., 2015; Salz et al., 2016), suggesting that the population of time cells is less able to distinguish times later in the interval. Similarly, the density of time fields decreases as a function of time (Kraus et al., 2013; Mello et al., 2015; Salz et al., 2016), having the same consequence on the ability to distinguish times later in the interval.

In this paper we report the results of analyses on the data-set initially reported in Kim et al., 2013. In particular, we study the cells that fired during circumscribed periods of time during the delay interval to determine if the mPFC contains a significant population of sequentially activated time cells and to determine if these cells code time in such a way that there is decreasing temporal accuracy as a function of time within the delay. This would suggest a connection with the hippocampal and striatal time code and demonstrate that the sequentially activated time cells are not specific to the hippocampus and striatum.

Methods

Behavioral tasks

As described in Kim et al., 2009 and Kim et al., 2013, three young male Sprague Dawley rats performed a temporal discrimination task on a modified T-maze (63 × 69 cm, elevated 30 cm from the floor; 8 cm wide track with 2.7 cm walls around the track except the central connecting bridge; see Figure 1A). Experiments were performed in the dark phase of 12 h light/dark cycle. The animals were required to discriminate six different durations of time intervals into short or long periods to obtain water reward. A new trial began when the animal came back from either goal location (Figure 1A, white circles) to the central arm via the lateral alley and broke the central photobeam (Figure 1A, arrow). The beginning of a time interval was signaled by a brief auditory tone when the animal broke the central photobeam. The end of a time interval was signaled by lowering the central bridge that allowed the animal to navigate to either goal location. The animals performed 164 to 273 (mean ± SD, 230 ± 20) trials per session. Six time intervals of different durations, which

63 were spaced evenly on a logarithmic scale, were presented in equal probability in random
64 order. The animal had to navigate to one designated goal (left, $n = 2$ animals; right, $n = 1$
65 animal) when a short (3018, 3310, or 3629 ms) interval was presented, and navigate to the
66 opposite goal when a long (3979, 4363, or 4784 ms) interval was presented to obtain water
67 reward. The animals were well-trained in the task by the time unit recordings began (see
68 Kim et al., 2009, for details). As reported in Kim et al., 2013 the animals chose the correct
69 target in 80% of trials. In the present study, we analyzed only the data recorded during the
70 delay intervals.

71 *Unit recording*

72 　　　As described in Kim et al., 2013 twelve tetrodes were chronically implanted in the
73 left or right mPFC (2.7 mm anterior and 0.7 mm lateral to bregma) and unit signals were
74 recorded from the dorsal anterior cingulate cortex, prelimbic cortex, and infralimbic cortex
75 (Figure 1B). Each animals' head position was monitored by tracking a set of light-emitting
76 diodes mounted on the headstage at 60 Hz. A total of 993 well isolated single units were
77 recorded, 791 of which were classified as putative pyramidal cells. Of these, we eliminated
78 260 units with mean firing rate < 1 Hz during the delay intervals. Additionally, in order
79 to restrict our attention to units with spike waveforms that were stable over the recording
80 sessions we eliminated 10 units with a difference of more than 10% in amplitude from the
81 first to the last 5 min of each session. A total of 723 units contributed to the subsequent
82 analyses.

83 *Classification of time cells*

84 　　　Kim et al., 2013 reported a population of units that started firing prior to the initiation
85 of the delay and decreased their firing as the delay proceeded and another population of
86 units that increased their firing monotonically during the delay interval. Both groups could
87 be responding to some event that preceded the delay interval or they could be predicting
88 an event that follows the delay interval. In the present analyses we restricted our attention
89 to units that both started and stopped firing within the delay interval on trials in which
90 the animal completed the task successfully.
91 　　　In order to evaluate to what extent the firing dynamics can be accounted for by
92 the elapse of time we computed the maximum likelihood fit of the spike train given the
93 Gaussian-shaped time fields as well as behavioral correlates: position and speed. The fit
94 was done on a spike train that included the activity during the delay intervals of all the
95 trials when the longest delay interval (4.784 ms) was presented. We restricted our attention
96 to the longest delay intervals so that we could observe the temporal dynamics for as long
97 as possible with this task. Given the duration of the delay intervals and the temporal
98 resolution of 1 ms for each trial we had a $N = 4784$ data points. If a spike was observed in
99 a particular 1 ms time bin, the corresponding data point was set to 1, otherwise it was set
100 to 0.
101 　　　We found the maximum likelihood of a spike train given the model with a set of
102 parameters Θ. The model $p\left(t, \vec{r}\left(t\right); \Theta\right)$ gives the probability of a spike at any given time
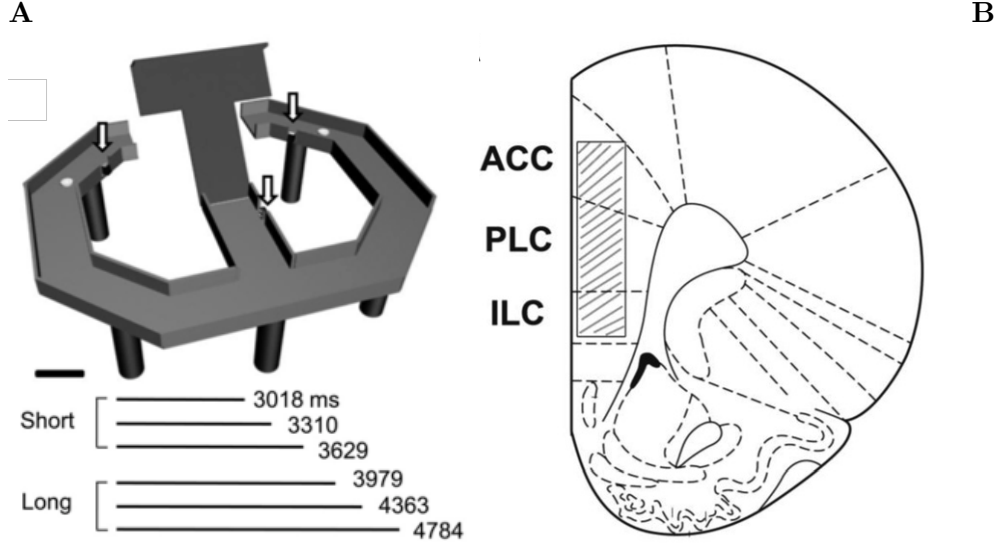103 point t:

A **B**

Figure 1. **A.** Behavioral task. Rats were tested on a figure 8-shaped maze to choose between two target locations (white circles) depending on the duration of a given time interval. A time interval began when the animal broke the central photobeam (arrow). The connecting bridge was lowered at the end of the time interval allowing the animal to proceed to either goal location. The bridge was elevated again when the animal broke a photobeam (arrow) at either goal location. Scale bar, 10 cm. **B.** Recording locations (shaded regions). The diagram is a coronal section view of the brain (2.7 mm anterior to bregma). Reproduced from Kim et al. (2013).

$$p\left(t, \vec{r}(t); \Theta\right) = a_1 + a_2 T + a_3 P + a_4 S + a_5 TP + a_6 TS + a_7 PS + a_8 TPS. \qquad (1)$$

The model takes into account the time $T(t; \sigma_t, \mu_t)$, the current position of the animal $P\left(\vec{r}(t); \vec{\sigma}, \vec{\mu}, \theta\right)$ and speed S, as well as their cross terms. Factors a_1 to a_8 determine the contribution of each of the terms, with a_1 being the constant term. The time term $T(t; \sigma_t, \mu_t)$ is a Gaussian-shaped time field defined as:

$$T(t; \sigma_t, \mu_t) = e^{\frac{-(t-\mu_t)^2}{2\sigma_t^2}}, \qquad (2)$$

where μ_t is a temporal shift of the peak of the time field and σ_t is a standard deviation of the time field. The position term $P\left(\vec{r}(t); \vec{\sigma}, \vec{\mu}, \theta\right)$ is a Gaussian-shaped elliptical place field defined as:

$$P\left(\vec{r}(t); \vec{\sigma}, \vec{\mu}, \theta\right) = e^{-(\alpha(x-\mu_x)^2 - 2\beta(x-\mu_x)(y-\mu_y) + \gamma(y-\mu_y)^2)}. \qquad (3)$$

In the above equation P is a function of $\vec{r}(t) = \{x(t), y(t)\}$, $\vec{\sigma} = \{\sigma_x, \sigma_y\}$ and $\vec{\mu} = \{\mu_x, \mu_y\}$. α, β and γ are functions of θ, $\vec{\sigma}$ and $\vec{\mu}$ as follows: $\alpha = \frac{cos^2(\theta)}{2\sigma_x^2} + \frac{sin^2(\theta)}{2\sigma_y^2}$, $\beta = \frac{-sin(2\theta)}{4\sigma_x^2} + \frac{sin(2\theta)}{4\sigma_y^2}$ and $\gamma = \frac{sin^2(\theta)}{2\sigma_x^2} + \frac{cos^2(\theta)}{2\sigma_y^2}$. $x(t)$ and $y(t)$ are the spatial coordinates of the animal's position

114 as a function of time, μ_x and μ_y are the spatial shifts of the peak of the place field in the x
115 and y direction respectively, σ_x and σ_y are the standard deviations of the place field, also
116 in the x and y direction respectively and θ is the angle of the place field.

117   The mean of the time term μ_t was allowed to vary between -100 ms and 4884 ms
118 and the standard deviation σ_t varied between 0 and 10 s. The upper bounds of the spatial
119 parameters were chosen such that they go well beyond the dimensions of the waiting area.
120 In order to obtain a probability of a spike at any time bin we had to ensure that the values
121 of $p\left(t, \vec{r}(t)\,; \Theta\right)$ are bounded between 0 and 1. Therefore the coefficients were bounded such
122 that $\sum_{i=1}^{8} a_i \leq 1$. The likelihood of the fit is defined as a product of these probabilities
123 across all $N = 4784$ time bins within each trial and across M trials. We expressed the
124 likelihood in terms of the negative log-likelihood (nLL), therefore instead of a product, a
125 sum of the probabilities was computed:

$$\underset{\Theta}{\arg\min}\ \text{nLL} = -\sum_{trial}\sum_{t}\left[f_t\ \log(p_t) + (1 - f_t)\log(1 - p_t)\right]. \tag{4}$$

126   To find the best fitting model the parameter space was iteratively searched using a
127 combination of particle swarming and the Quasi-Newton method. Particle swarming was
128 performed first (with the swarm size equal to 50) and its output was used to initialize
129 the Quasi-Newton method which was performed second (the number of maximum function
130 evaluations was set to 10000). The computations were implemented in Matlab 2015b. To
131 avoid solutions that converge to a local minimum, the fitting procedure was repeated until
132 the algorithm did not result with better likelihood for at least 20 consecutive runs.

133   In order to quantify whether the contribution of the terms that contained time was
134 significant, the maximum log-likelihood was computed again, but this time by setting those
135 four time related terms to zero (a_2, a_5, a_6, a_8 equal to zero). So only: a_1, a_3, a_4, a_7, σ, μ and
136 θ had to be estimated. Since the models with and without time are nested, the likelihood-
137 ratio test was used to asses the probability that adding the time terms significantly improves
138 the fit. To assure that a cell will not be classified as a time cell only due to its activity in a
139 single trial, the analysis was done separately on even and odd trials. For a cell to be classified
140 as a time cell it was required that the likelihood-ratio test was significant ($p < 0.05$) for
141 even and odd trials. In order eliminated cells with ramping or decaying firing rate during
142 a delay interval, μ_t was required to be within the delay interval and at least one σ_t away
143 from either the beginning or the end of the interval. Also, to eliminate cells with overly
144 flat firing rate, σ_t was required to be at most equal to the length of the delay interval. To
145 ensure reproducibility, the entire fitting procedure was done twice and exactly the same set
146 of cells was classified as time cells in both runs.

147   Results

148 *Sequentially activated time cells exist in mPFC*

149   We identified a subpopulation of sequentially activated cells that fired at a consistent,
150 circumscribed time during delay intervals (Figure 2). These mPFC units appear to have
151 firing correlates that resemble time cells observed in the hippocampus (Kraus et al., 2013;
152 Gill et al., 2011; MacDonald et al., 2011; Pastalkova et al., 2008; Modi, Ashesh, & Bhalla,

2014) and striatum (Mello et al., 2015; Adler et al., 2012). A total of 73/723 units were classified as time cells.

First, we note informally that the population of time cells decreased in its temporal accuracy as time during the interval proceeds. Figure 4A and Figure 4C show the ensemble similarity (cosine of the normalized firing rate vectors) of the population of time cells between all pairs of time points during the delay period (in Figure 4C the firing that could be explained with position and speed) was subtracted from the overall firing rate). This finding replicates the conclusions of Kim et al., 2013 but restricting attention to the population of time cells. Further analyses revealed two causes for the decrease in temporal accuracy. These can be read off from Figure 4B which shows the temporal profile of all 73 units classified as time cells, sorted by the peak time of the estimated Gaussian shaped time fields (μ_t), Again, similar results were obtained with only the firing that could not be explained by position and speed (Figure 4D).

The width of firing fields increased with the passage of time. The width of the central ridge in Figure 4B and Figure 4D increases from the left of the plot to the right of the plot. This suggests that units that elevated firing rate earlier in the delay interval tend to have narrower time fields than the units that fire later in the delay interval. This impression was confirmed by analyses of the across-units relationship between the peak time (μ_t) and the standard deviation (σ_t) of the estimated Gaussian shaped time fields across time cells (Figure 3A). The correlation between the peak time and the width was significant (Pearson's correlation 0.52, $p < 10^{-5}$). Linear regression model linking the peak time (independent variable) and the width (dependent variable) resulted with a significant intercept equal to 0.27 ± 0.07 (SE) with $p < 0.001$ and a significant slope equal to 0.18 ± 0.04 (SE) with $p < 10^{-5}$.

Increase of the width of the time fields with the peak time was not an artifact of trial averaging. The property of spreading time fields seen in Figure 4 could be an averaging artifact caused by trial to trial variability. To show that this was unlikely to be the case we found the maximum likelihood fit for each trial independently. Prior to the fitting procedure all the parameters except μ_t and σ_t were fixed to the values found through the fit of the entire spike train spanning all the trials. The trial-averaged μ_t and σ_t were still significantly correlated (Pearson's correlation 0.42, $p < 10^{-3}$). This suggests that the dynamics of the spreading time fields is noticeable on a trial level as well. The trial-averaged and global (used in the previous analysis) μ_t and σ_t were significantly correlated (Pearson's correlation 0.80, $p < 10^{-16}$ for μ_t and 0.83, $p < 10^{-18}$ for σ_t).

Later times are represented by fewer cells than earlier times. The population of cells covered the entire delay interval, but not evenly. The number of cells with peak firing later in the interval was smaller than the number of cells with peak firing earlier in the interval. This can be seen from the fact that the central ridge does not follow a straight line, as would have been expected of a uniform distribution of peak times (μ_t), but flattens as the interval proceeds. To quantify this, we examined the distribution of the peak times across time cells (Figure 3B). The KS test rejected the hypothesis that the distribution of the peak times is uniform (KS test $D(73) = 0.63$, $p < 10^{-12}$).
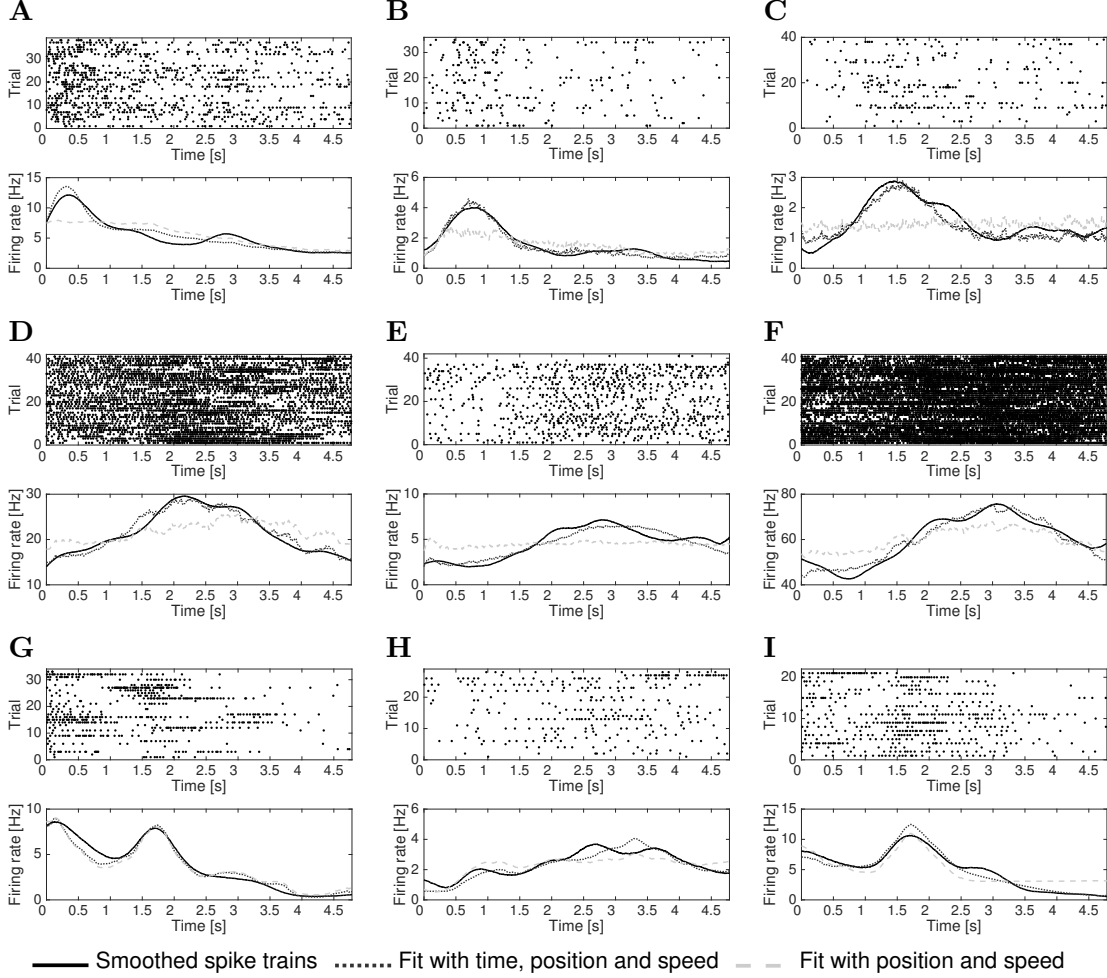
Figure 2. Firing properties of several time-modulated mPFC cells during the longest delay interval and the model fits with and without the temporal terms. Top two rows (**A** to **F**): examples of cells classified as time cells. The model that includes time component fits the spike train significantly better than the model that includes only position and speed. Bottom row (**G** to **I**): examples of cells that were not classified as time cells because behavioral correlates could account for the temporally modulated firing. Adding the time component to the model did not improve the fit significantly as compared to the model that contained only position and speed, despite the temporal modulation of the cells activity.. Each of the nine plots (**A-I**) displays activity of a single cell. On each plot the top row shows raster plots where each dot denotes a spike and the bottom row shows the averaged trial activity (solid line). Only trials when the animal made a correct choice are shown. The onset of the delay interval is at zero and the end at 4.784 s. The cells **A** to **F** are ordered such that the esimated peak time (μ_t) increases progressively from the first to the sixth cell.
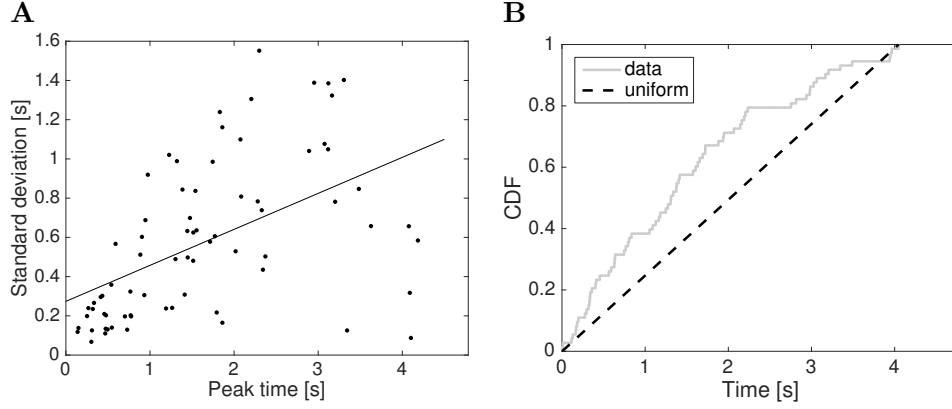
Figure 3. Sequentially activated time cells in mPFC encode time in a gradually decreasing fashion: 1) width of the time fields increases with the peak time (plot **A**, each dot represent a single time cell and the line is a least square fit linear fit without a constant term) and 2) peak times of the time fields are non-uniformly distributed along the delay interval, more cells had time fields earlier in the delay interval than later in the delay interval (plot **B**).

¹⁹⁵ *Comparing time cells in different subregions of the mPFC.* We compared the time
¹⁹⁶ cells based on the subregion of the mPFC where they were recorded. The subregions that
¹⁹⁷ were considered were dorsal anterior cingulate cortex (dACC), prelimbic cortex (PLC), and
¹⁹⁸ infralimbic cortex (ILC). The number of cells classified as time cells in dACC was 19 out
¹⁹⁹ of 120, in PLC 47 out of 426 and in ILC 7 out of 187. The proportion of time cells was not
²⁰⁰ significantly different between dACC and PLC (Fisher's exact test $p > 0.15$, two-tailed),
²⁰¹ but it was significantly smaller in ILC with respect to both dACC (Fisher's exact test
²⁰² $p < 0.001$, two-tailed) and PLC (Fisher's exact test $p < 0.01$, two-tailed). Distributions of
²⁰³ μ_t and σ_t did not significantly differ across the three subregions (Kruskal-Wallis test, for
²⁰⁴ μ_t: H = 1.86, d.f. = 2, p = 0.39; for σ_t: H = 2.31, d.f. = 2, p = 0.31).

²⁰⁵ *The firing fields share qualitative properties across the delay intervals of different*
²⁰⁶ *duration.* The animals were presented with six different delay intervals. In Figure 4E the
²⁰⁷ same type of a heatplot as on Figure 4B is shown, but for all 6 delay intervals when the
²⁰⁸ animal made a correct choice (top row) and when the animal made an incorrect choice
²⁰⁹ (bottom row). The cells are ordered in the same way as on Figure 4B. In general, the
²¹⁰ firing dynamics appeared to be abruptly interrupted once the end of the delay interval was
²¹¹ signaled. The firing fields appear qualitatively similar regardless of the length of the delay
²¹² interval or whether the animal made a correct or incorrect choice. Not enough error trials
²¹³ were available for a statistical comparison, especially at the extreme intervals.

²¹⁴ *mPFC time cells and ramping cells convey comparable amount of temporal informa-*
²¹⁵ *tion.* We quantified how well the mPFC neuronal ensemble kept track of time. The longest
²¹⁶ time interval (4784 ms) was divided into 10 equal-duration bins and the order of the middle
²¹⁷ eight bins was decoded based on neural activity within each bin using linear discriminant
²¹⁸ analysis (Kim et al., 2013). We compared the results on different populations of cells: all
²¹⁹ 723 cells (Figure 5A), all 73 time cells (Figure 5B) and 73 ramping cells (selected randomly
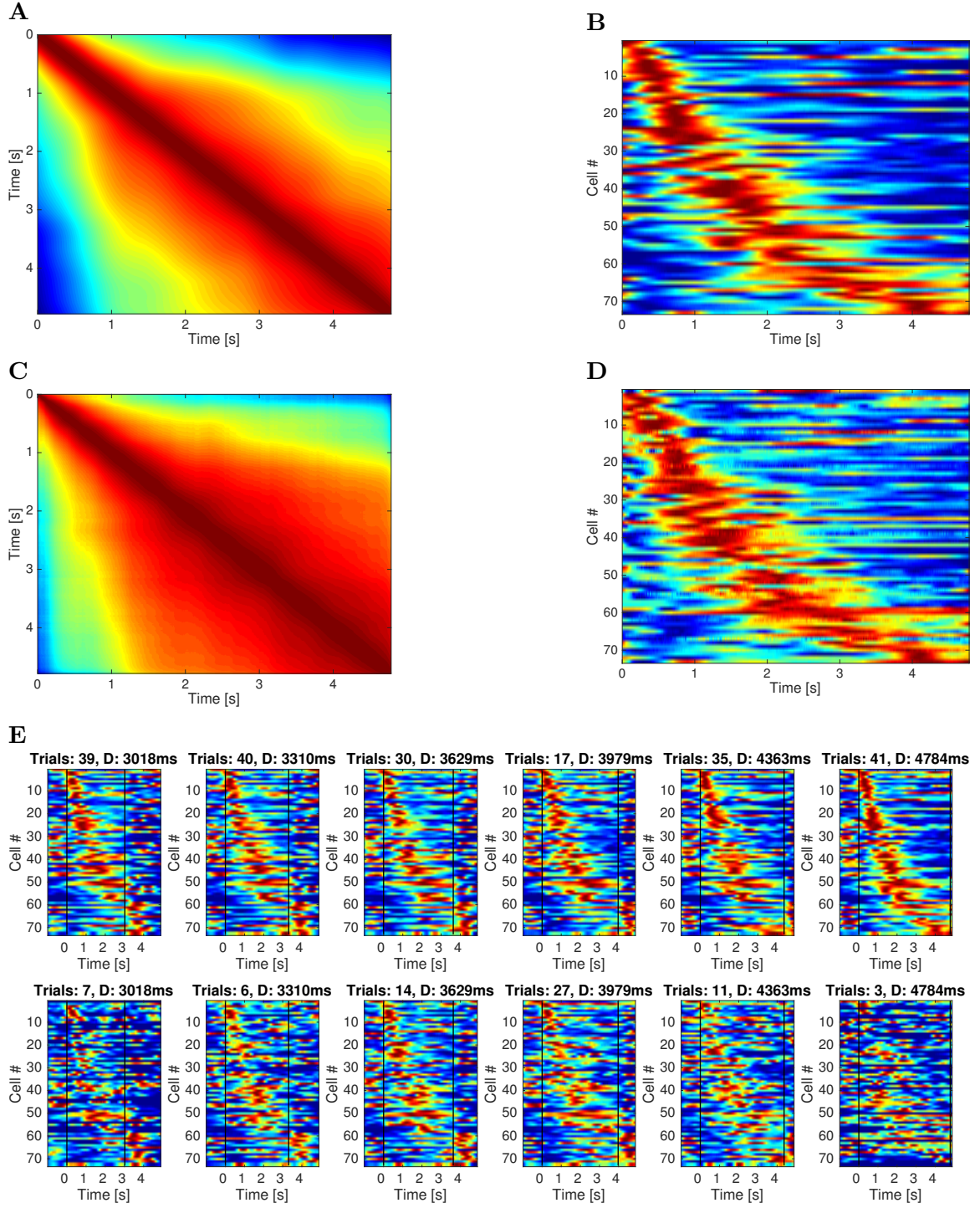
Figure 4. (Caption on the next page.)

Figure 4.   mPFC time fields show decreasing temporal accuracy for events further in the past. **A.** Ensemble similarity of all 73 time cells given through a cosine of the angle between normalized firing rate population vectors. The angle is computed at all pairs of time points during the delay period. The bins along the diagonal are necessarily one (warmest color). The similarity spreads out indicating that the representation changes more slowly later in the delay period than it does earlier in the delay period. **B.** Activity of all 73 time cells during the longest delay interval. Each row on the heatplot corresponds to a single cell and displays the firing rate (normalized to 1) averaged across all correct trials the animals performed during the longest delay interval. Red corresponds to high firing rate, while blue corresponds to low firing rate. The cells are sorted with respect to the peak time of the estimated Gaussian shaped time fields (μ_t). There are two features related to temporal accuracy that can be seen from examination of this plot. First, time fields later in the delay are more broad than time fields earlier in the delay. This can be seen as the widening of the central ridge as the peak moves to the right. In addition the peak times of the time cells were not evenly distributed across the delay, with later time periods represented by fewer cells than early time periods. This can be seen in the curvature of the central ridge; a uniform distribution of time fields would manifest as a straight line. **C.** and **D.** Same as **A** and **B** respectively, but only a part of the firing rate that was not accounted for by the behavioral correlates (position and speed) was used. **E.** Same as **A**, but for all the delay intervals when the animals made a correct choice (top row) or incorrect choice (bottom row). Vertical black lines mark the beginning (at time 0) and the end of a delay interval. Title of each heatplot contains a number of trials that the animals made in a particular condition. End of the delay interval seems to cause an abrupt change in the firing properties among the cells that were active at the time. Apart from that, there is no apparent qualitative difference among the 12 cases that could be attributed to either duration of the delay interval or to the correct or incorrect performance.

from a total of 228 cells that exhibit ramping firing rate, Figure 5C). The mean error in the prediction of elapsed time was similar for all three populations. This suggests that populations of time cells and ramping cells can convey roughly the same amount of information about the elapse of time.

Discussion

This study shows that mPFC contains sequentially activated time cells, similar to those previously reported in the hippocampus and striatum. As evaluated through ML fit, the findings were not attributable to confounds with position nor speed during the delay. The time fields of these units spanned the entire 5 s delay interval, but with temporal accuracy that decreased as time elapsed. The width of the time fields increased with temporal distance from the onset of the delay period and the distribution of the firing rate peaks strongly deviated from the uniform such that more units represented time periods early in the delay than later in the delay. These findings were not a result of a trial averaging artifact; rather the relationship between width and time was observed within single trials.

A common representational motif for time in the mPFC, hippocampus and striatum

Our findings add to a literature on temporally-modulated firing. Over longer scales, extensive evidence shows that the pattern of firing changes gradually over long periods of time in the hippocampus (Manns, Howard, & Eichenbaum, 2007; Mankin et al., 2012; Mankin, Diehl, Sparks, Leutgeb, & Leutgeb, 2015) and mPFC (Hyman, Ma, Balaguer-
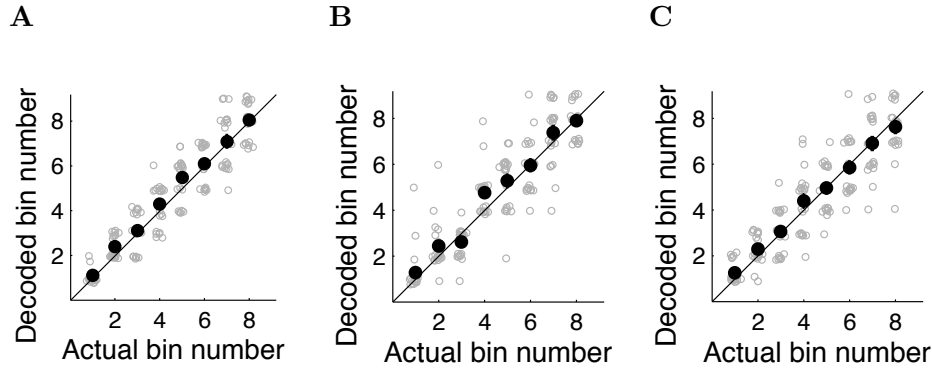
Figure 5. Population of mPFC time cells carried similar amount of temporal information as a same-size population of ramping cells. Decoded bin number versus actual bin number. Open gray circles denote the trial-by-trial decoding results for each bin. Filled black circles and error bars denote their means and SEM across trials. **A.** Temporal decoding based on all 723 reported units. Mean error: 0.71 bins. **B.** Temporal decoding based on all 73 time cells Mean error: 0.74 bins. **C.** Temporal decoding based on the randomly chosen 73 ramping cells. Mean error: 0.81 bins.

Ballester, Durstewitz, & Seamans, 2012). This paper reports that mPFC contained sequentially activated time cells with decreasing temporal accuracy over shorter time scale. Several previous studies have found cells that fire for circumscribed periods of time during delay intervals in the hippocampus (MacDonald et al., 2011; Salz et al., 2016; Gill et al., 2011; Kraus et al., 2013; MacDonald, Carrow, Place, & Eichenbaum, 2013; Modi et al., 2014; Naya & Suzuki, 2011; Pastalkova et al., 2008) and the striatum (Mello et al., 2015; Adler et al., 2012). Many of these studies have observed decreasing temporal accuracy as a function of delay, due to spread in time field width (Howard et al., 2014; Mello et al., 2015; Adler et al., 2012; Kraus et al., 2013; Salz et al., 2016) and/or due to a non-uniform distribution of time field locations (Kraus et al., 2013; Salz et al., 2016; Mello et al., 2015). Despite differences in the procedures of the experiments, including variations in the behavioral task, the species, and the recording techniques, these remarkably consistent qualitative properties suggest a common motif for representation of time across these regions. In particular, resolution for the time of past events decreases with the passage of time. Notably, decreasing temporal resolution with the passage of time is a hallmark of behavioral findings from both timing tasks (Wearden & Lejeune, 2008; Lewis & Miall, 2009; Gibbon, 1977) and a wide range of memory tasks across species (Gallistel & Gibbon, 2000; Howard, Shankar, Aue, & Criss, 2015).

Mechanisms that could generate time cells

       Time of the peak firing rate of the time cells typically exceeds the time constants of ion channels and neural processes, such as calcium clearance, which are both in general below 1 s. Several studies have proposed that neural firing with long time constants could be a result of feedback mechanisms at the single neuron level (Tiganj, Hasselmo, & Howard, 2015; Shouval & Gavornik, 2011). For instance, one action potential could trigger the next through neuron-level processes that occur during action potential generation, such as

calcium influx. Network-based mechanisms that can result in long time constants were also proposed (e.g., Gavornik & Shouval, 2011; Simen, Balci, de Souza, Cohen, & Holmes, 2011; Major & Tank, 2004; Brody, Romo, & Kepecs, 2003; Bernacchia, Seo, Lee, & Wang, 2011). Gradually changing firing rates with long time constants can be converted into time fields through a mechanism that resembles lateral inhibition (Howard et al., 2014). The mechanism would require two layer feed-forward network to construct time cells, which are not mutually connected. Alternatively, sequential activation (Itskov, Curto, Pastalkova, & Buzsáki, 2011; Jensen & Lisman, 1996; Hasselmo, 2009; Tieu, Keidel, McGann, Faulkner, & Brown, 1999) could as well give rise to time cells. Spectral timing could also give rise to time cells (Grossberg & Merrill, 1992; Grossberg & Schmajuk, 1989). In general, proposed mechanisms should account for the qualitative properties observed here and in other studies: non-uniform distribution of the times of the peak firing rate and spread of the firing fields.

Concluding remarks

Previous work has shown that neural ensembles in the rodent mPFC code time with decreasing temporal accuracy (Kim et al., 2013). This paper extends these findings and reports that a subpopulation of units in the mPFC fired like sequentially activated time cells, firing for circumscribed periods of time during the delay of an interval discrimination task. These time cells exhibited decreasing temporal accuracy in two ways. First, time cells that fired later in the delay interval had wider temporal receptive fields than time cells that fired earlier in the delay. Second, the distribution of time fields was not uniform. More cells had time fields earlier in the delay period than later in the delay period. Taken together, these findings are consistent with the hypothesis that the mPFC is part of a system that represents time with decreasing accuracy over a scale of seconds.

References

Adler, A., Katabi, S., Finkes, I., Israel, Z., Prut, Y., & Bergman, H. (2012). Temporal convergence of dynamic cell assemblies in the striato-pallidal network. *Journal of Neuroscience*, *32*(7), 2473-84. doi: 10.1523/JNEUROSCI.4830-11.2012

Bernacchia, A., Seo, H., Lee, D., & Wang, X. J. (2011). A reservoir of time constants for memory traces in cortical neurons. *Nature Neuroscience*, *14*(3), 366-72.

Brody, C. D., Romo, R., & Kepecs, A. (2003). Basic mechanisms for graded persistent activity: discrete attractors, continuous attractors, and dynamic representations. *Current Opinion in Neurobiology*, *13*(2), 204–211.

Buhusi, C. V., & Meck, W. H. (2005). What makes us tick? Functional and neural mechanisms of interval timing. *Nature Reviews Neuroscience*, *6*(10), 755-65. doi: 10.1038/nrn1764

Gallistel, C. R., & Gibbon, J. (2000). Time, rate, and conditioning. *Psychological Review*, *107*(2), 289-344.

Gavornik, J. P., & Shouval, H. Z. (2011). A network of spiking neurons that can represent interval timing: mean field analysis. *Journal of Computational Neuroscience*, *30*(2), 501-13. doi: 10.1007/s10827-010-0275-y

Gibbon, J. (1977). Scalar expectancy theory and Weber's law in animal timing. *Psychological Review*, *84*(3), 279-325.

Gill, P. R., Mizumori, S. J. Y., & Smith, D. M. (2011). Hippocampal episode fields develop with learning. *Hippocampus*, *21*(11), 1240-9. doi: 10.1002/hipo.20832

Grossberg, S., & Merrill, J. (1992). A neural network model of adaptively timed reinforcement learning and hippocampal dynamics. *Cognitive Brain Research*, *1*, 3-38.

Grossberg, S., & Schmajuk, N. (1989). Neural dynamics of adaptive timing and temporal discrimination during associative learning. *Neural Networks*, *2*(2), 79–102.

Hasselmo, M. E. (2009). A model of episodic memory: Mental time travel along encoded trajectories using grid cells. *Neurobiology of Learning and Memory*, *92*, 559-73.

Howard, M. W., MacDonald, C. J., Tiganj, Z., Shankar, K. H., Du, Q., Hasselmo, M. E., & Eichenbaum, H. (2014). A unified mathematical framework for coding time, space, and sequences in the hippocampal region. *Journal of Neuroscience*, *34*(13), 4692-707. doi: 10.1523/JNEUROSCI.5808-12.2014

Howard, M. W., Shankar, K. H., Aue, W., & Criss, A. H. (2015). A distributed representation of internal time. *Psychological Review*, *122*(1), 24–53. doi: 10.1037/a0037840

Hyman, J. M., Ma, L., Balaguer-Ballester, E., Durstewitz, D., & Seamans, J. K. (2012). Contextual encoding by ensembles of medial prefrontal cortex neurons. *Proceedings of the National Academy of Sciences USA*, *109*, 5086-91. doi: 10.1073/pnas.1114415109

Itskov, V., Curto, C., Pastalkova, E., & Buzsáki, G. (2011). Cell assembly sequences arising from spike threshold adaptation keep track of time in the hippocampus. *Journal of Neuroscience*, *31*(8), 2828-34.

Jensen, O., & Lisman, J. E. (1996). Hippocampal CA3 region predicts memory sequences: Accounting for the phase precession of place cells. *Learning and Memory*, *3*, 279-287.

Kim, J., Ghim, J.-W., Lee, J. H., & Jung, M. W. (2013). Neural correlates of interval timing in rodent prefrontal cortex. *Journal of Neuroscience*, *33*(34), 13834-47. doi: 10.1523/JNEUROSCI.1443-13.2013

Kim, J., Jung, A. H., Byun, J., Jo, S., & Jung, M. W. (2009). Inactivation of medial prefrontal cortex impairs time interval discrimination in rats. *Frontiers in Behavioral Neuroscience*, *3*.

Kraus, B. J., Robinson, R. J., 2nd, White, J. A., Eichenbaum, H., & Hasselmo, M. E. (2013). Hippocampal "time cells": time versus path integration. *Neuron*, *78*(6), 1090-101. doi: 10.1016/j.neuron.2013.04.015

Lejeune, H., & Wearden, J. H. (2006). Scalar properties in animal timing: conformity and violations. *Quarterly Journal of Experimental Psychology*, *59*(11), 1875-908.

Lewis, P. A., & Miall, R. C. (2009). The precision of temporal judgement: milliseconds, many minutes, and beyond. *Philosophical Transcripts of the Royal Society London B: Biological Sciences*, *364*(1525), 1897-905. doi: 10.1098/rstb.2009.0020

MacDonald, C. J., Carrow, S., Place, R., & Eichenbaum, H. (2013). Distinct hippocampal time cell sequences represent odor memories immobilized rats. *Journal of Neuroscience*, *33*(36), 14607–14616.

MacDonald, C. J., Lepage, K. Q., Eden, U. T., & Eichenbaum, H. (2011). Hippocampal "time cells" bridge the gap in memory for discontiguous events. *Neuron*, *71*, 737-749.

Major, G., & Tank, D. (2004). Persistent neural activity: prevalence and mechanisms. *Current Opinion in Neurobiology*, *14*(6), 675-84. doi: 10.1016/j.conb.2004.10.017

Mangels, J. A., Ivry, R. B., & Shimizu, N. (1998). Dissociable contributions of the prefrontal and neocerebellar cortex to time perception. *Cognitive Brain Research*, *7*(1).

Mankin, E. A., Diehl, G. W., Sparks, F. T., Leutgeb, S., & Leutgeb, J. K. (2015). Hippocampal CA2 Activity Patterns Change over Time to a Larger Extent than between Spatial Contexts. *Neuron*, *85*(1), 190–201.

Mankin, E. A., Sparks, F. T., Slayyeh, B., Sutherland, R. J., Leutgeb, S., & Leutgeb, J. K. (2012). Neuronal code for extended time in the hippocampus. *Proceedings of the National Academy of Sciences*, *109*, 19462-7. doi: 10.1073/pnas.1214107109

Manns, J. R., Howard, M. W., & Eichenbaum, H. B. (2007). Gradual changes in hippocampal activity support remembering the order of events. *Neuron*, *56*(PMC2104541), 530-540.

Mello, G. B. M., Soares, S., & Paton, J. J. (2015). A Scalable Population Code for Time in the Striatum. *Current Biology*, *25*(9), 1113–1122.

359 Modi, N. M., Ashesh, D. K., & Bhalla, S. U. (2014). CA1 cell activity sequences emerge after reor-
360   ganization of network correlation structure during associative learning. *eLife*, *3*(0). Retrieved
361   from `http://dx.doi.org/10.7554/eLife.01982` doi: 10.7554/eLife.01982
362 Naya, Y., & Suzuki, W. (2011). Integrating what and when across the primate medial temporal
363   lobe. *Science*, *333*(6043), 773-776.
364 Onoe, H., M., K., Onoe, K., Takechi, H., Tsukada, H., & Watanabe, Y. (2001). Cortical net-
365   works recruited for time perception: A monkey positron emission tomography (pet) study.
366   *NeuroImage*, *13*(1), 37 - 45.
367 Pastalkova, E., Itskov, V., Amarasingham, A., & Buzsaki, G. (2008). Internally generated cell
368   assembly sequences in the rat hippocampus. *Science*, *321*(5894), 1322-7.
369 Salz, D. M., Tiganj, Z., Khasnabish, S., Kohley, A., Sheehan, D., Howard, M. W., & Eichenbaum,
370   H. (2016). Time cells in hippocampal area CA3. *The Journal of Neuroscience*, *In press*.
371 Shouval, H. Z., & Gavornik, J. P. (2011). A single spiking neuron that can represent interval timing:
372   analysis, plasticity and multi-stability. *Journal of Computational Neuroscience*, *30*(2), 489-99.
373   doi: 10.1007/s10827-010-0273-0
374 Simen, P., Balci, F., de Souza, L., Cohen, J. D., & Holmes, P. (2011). A model of in-
375   terval timing by neural integration. *Journal of Neuroscience*, *31*(25), 9238-53. doi:
376   10.1523/JNEUROSCI.3121-10.2011
377 Tieu, K. H., Keidel, A. L., McGann, J. P., Faulkner, B., & Brown, T. H. (1999). Perirhinal-amygdala
378   circuit level computational model of temporal encoding in fear conditioning. *Psychobiology*,
379   *27*, 1-25.
380 Tiganj, Z., Hasselmo, M. E., & Howard, M. W. (2015). A simple biophysically plausible model for
381   long time constants in single neurons. *Hippocampus*, *25*(1), 27-37.
382 Wearden, J. H., & Lejeune, H. (2008). Scalar properties in human timing: conformity and violations.
383   *Quarterly Journal of Experimental Psychology*, *61*(4), 569-87.